sciendo **Transactions on Aerospace Research** eISSN 2545-2835, VOL. 268, NO. 3/2022, 74-90
DOI: 10.2478/tar-2022-0018

TECHNIQUE USED TO PERFORM ROCKET-PLANE FREE-FLIGHT TESTS

Agnieszka Kwiek[1*], **Krzysztof Bogdański**[1], **Jarosław Hajduk**[2], **Andrzej Tarnowski**[1]
[1] Aircraft Design Division, Institute of Aeronautics and Applied Mechanics,
Warsaw University of Technology, Nowowiejska 24, 00-665, Warsaw, Poland
[2] Airplane and Helicopter Department, Air Force Institute of Technology,
Księcia Bolesława 6, 01-494, Warsaw, Poland

Abstract

This paper includes description of the technique that was applied for free-flight (drop) tests of the rocket-plane scaled model. The main aim of the experiment was to validate the numerical approach to be used to simulate the gliding flight of the rocket-plane, especially the transition between high to low angles of attack and the rocket-plane response to control. The primary goal of this paper is to show what kind of challenges must be addressed when planning the flight test campaign. This paper includes description of how the rocket-plane model was scaled and built, the model preparation, experimental design and flight procedure. This paper shows an overview of how the experiment can be planned for different scenarios and the lessons learned during the deep stall free-flight tests.

Keywords: aerospace engineering; drop tests; free-flight test; rocket-plane
Type of the work: research article

1. INTRODUCTION

Numerical software, even very sophisticated ones, use mathematical models that are created based on some sets of assumptions. This means that they include some sort of simplifications of the real world. On the other hand, solving a multidisciplinary problem might generate a problem with convergence, or the time of numerical model preparation and computation might exceed the effort required to carry out the experiment to collect the needed data. There is also uncertainty whether the numerical model can correctly predict the aerodynamics, for instance, when there is a strong separation. Therefore, experiments on models or prototypes are an integral part of both aircraft and spacecraft design process and certification process. Nevertheless, conducting the experiment usually is also linked with some assumptions, especially if the experiment is conducted on the scaled model not on the fully functional prototype. In that case, the preparation of the experimental model and the experiment itself are strongly related with the type of the data that are planned to be collected. On the other hand, in the early stages of the project of unconventional aircraft, conducting simple experiments to validate low-fidelity numerical packages can be more effective than using complex numerical methods. Moreover, the cost of conducting numerical simulations that need to take into account strong nonlinearity might be higher than to carry out a simple experiment to validate a numerical approach. This seems to be more effective for unconventional designs.

This paper considers a rocket-plane that is designed for suborbital manned space flights [1–3]. The rocket-plane is designed with a tailless configuration and is launched from a carrier that is also

* Corresponding Author: Agnieszka Kwiek, agnieszka.kwiek@pw.edu.pl
ARTICLE HISTORY **Received** 2022-02-02 **Revised** 2022-04-04 **Accepted** 2022-06-20

designed in a tailless configuration (see Fig. 1). When both vehicles are coupled together, they create a conventional aircraft, wherein the rocket-plane's wing works as the empennage. The mission profile of the system assumes that the rocket-plane is carried by the carrier up to 15 km above the sea level, and then the vehicles separate. The carrier returns to the airport, while the rocket-plane begins the flight on the parabola-shaped trajectory. First, the rocket engine is used to accelerate the rocket-plane; then, the engine is shut down and the rocket-plane continues the mission until it reaches the apogee. Next, the process of reentry begins; during this phase, the rocket-plane slows down by utilising the vortex lift generated by the leading edge extension (LEX). Before the landing, the rocket-plane must transit from a flight on high angles of attack to low angles of attack.

Figure 1. The carrier (light grey) and the rocket-plane (dark grey) flying in coupled configuration [own study].

Both the separation process and the reentry involve a flight in a deep stall; therefore, the way to validate a numerical simulation must be addressed. In this paper, a technique used in the planning and preparation of a free-flight experiment that can be used to validate a numerical package for flight simulation (Simulation and Dynamic Stability Analysis [SDSA] package) is presented.

2. METHOD

2.1. Experimental requirements

The aim of the experiment is to conduct the free-flight (unpowered) test of the rocket-plane that must be dropped at a speed lower than the stall speed. The experiment investigates a flight in a deep stall condition and the transition from high angles of attack to low angles of attack. During the transition, high g-loads are expected because this rocket-plane is designed for manned tourist flights. The Federal Aviation Administration (FAA) recommendation regarding the maximum-allowed g-loads must be met [4]. Therefore, measurement of the g-loads must be planned. The collected data should include the angle of attack (AoA), airspeed, position of the control surfaces and the g-loads. Due to the early design stage, the experiment must be designed as a low-cost one without access to a professional airfield. The experimental cost and early stage of the design also imply that the model is going to be controlled manually by an operator on the ground and that all flights must be performed within line of sight of the ground operator.

2.2. Scaling a model

Before the flight tests can be carried out, the suitable model, flight conditions and technique of an experiment must be selected. Typically, a flight test is a technique for the validation of the aircraft behaviour or validation that the aircraft meets the design and certification requirements [5,6]. Such a test is conducted using either a dynamic scaled model or a full-scale prototype [7,8]. The scaled model allows reducing the cost of tests due to a lower cost of the model's manufacture and the lower operational costs

of an experimental infrastructure. In terms of using the scaled model, it must be scaled according to proper similarity numbers [9]. Depending on the kind of tests needed, the selection of the similarity numbers may vary. The decision process related to which of those similarity numbers must be met is linked with the phenomenon that drives the tested behaviour or those that can be neglected due to an insignificant impact. Usually, it is one of the following approaches—Mach scaling or Froude scaling [7,9]. Fulfilling all similarity numbers simultaneously is not possible because that would require meeting excluding conditions. In the case of the aircraft drop (free-flight) test, when the flow can be assumed as an incompressible one, the model should be scaled according to the Froude scale (Table 1).

Table 1. Scaling factors for Froude's scaling in the case of incompressible flow.

Parameter	**Expression**
Linear dimension (l_{model} /$l_{aircraft}$)	n
Relative density	$m/\rho l^3$
Froude number (Fr_{model} /$Fr_{aircraft}$)	1
Acceleration due to gravity ($g_{model}/g_{aircraft}$)	1
Angle of attack	1
Mass	n^3/σ
Moment of inertia	n^5/σ
Linear velocity	$n^{1/2}$
Angular velocity	$1/n^{1/2}$
Time	$n^{1/2}$
Reynolds number	$n^{3/2}\ \upsilon_{mode}/\upsilon_{aircraft}$
where $\sigma = \rho_{model}/\rho_{aircraft}$	

In terms of the rocket-plane tests, a few challenges must be addressed. First, the flight test altitude needs to be selected, which is directly related to the acceleration due to gravity and the air density. According to the Froude number, the ratio of acceleration due to gravity to the altitude of the nominal flight level and the scaled model test flight level must be equal to one. The ratio of the acceleration due to gravity for the case of H = 0 km and H = 15 km is very close to the ratio between acceleration due to gravity on the equator and the pole, respectively; therefore, for the considered test, it seems to be reasonable to assume that even performing the experiment at an altitude close to the ground meets the mentioned condition. The next challenge that is related to fulfilling the Froude scale is associated with the air density, which directly affects the model's mass. For the considered case, the mass of the scaled model that meets the Froude scale for flight tests near the ground is almost 15 kg. Such a heavy model would be very difficult to control due to the testing at low altitude and at a high descent rate. On the other hand, the model that has a reasonable weight in terms of design and control must be tested at very high altitude, >12 km, which is not feasible in the case of the remote-control models when the pilot (operator) is standing on the ground and manually controlling the aircraft model. Finally, due to the early stage of the design and the desire to conduct a low-cost experiment, the Froude scaling is not met. The approach for analysis of the aircraft behaviour was a hybrid between experimental and numerical tests. In this paper, flight tests of a geometrically scaled model (but not a dynamically scaled model) were carried out. The data collected during the experiment were used in software validation to ensure that

the numerical simulation can predict such an unusual mission in a reliable way. The software, i.e., SDSA package [10], has been already verified for conventional aircrafts [11] and unconventional aircraft flying on low AoA [12,13] but not validated for the case when the aircraft is flying in a deep stall condition. This paper focuses on presentation of the flight test campaign preparation and the technique of performing the free-flight tests. The presentation and analysis of the data measured during those free flights can be found elsewhere [14].

2.3. Takeoff technique

Depending on the test purpose, aircraft size and aircraft design, a model can take off (launch) in different ways. The most common approaches are regular takeoff, catapult and drop. In the case of the regular takeoff, the aircraft model must be equipped with a classic landing gear and engine [8,15–18], which usually are not suitable for glide (unpowered flight) tests. Moreover, this can affect the results, e.g., by adding extra drag component due to the existence of a propeller. On the other hand, building a model with a retractable landing gear or propulsion system makes the model unnecessarily more complex. Furthermore, the considered rocket-plane is not designed for standard takeoff. The second approach utilises a bungee cord [13]; in such a case, the aircraft is accelerated by the energy stored in the stretched elastic cord. However, this is mostly applicable for quite small aircraft models with a low stall speed that are equipped with an engine. For this technique, where the engine is located is important and is not always convenient for the aircraft in pusher configuration with a propeller installed at the back. The third approach is using a catapult, but this implicates that g-forces act on the aircraft, which are going to be higher and require a more rigid airframe structure [19]. However, the stall speed can be higher than that while using a simple bungee cord. Again, this approach is applicable in the case of aircraft equipped with a propulsion system, but this solution can be more convenient if the propeller is installed at the back. None of the above-listed approaches is appropriate for free-flight tests of the considered rocket-plane. The last option is to drop an aircraft from a carrier, which—for the considered experiment—is the most suitable approach [20–25]. However, the next question that must be addressed is what kind of vehicle should be used as a carrier. In general, four different types of carriers can be distinguished: aircraft, helicopter, balloon and kite. The first two are quite often used in flight tests, including tests with a prototype. Balloons are popular for supersonic vehicle tests, while according to the authors' knowledge, a kite has not been used as a carrier in scientific research yet.

In the case of the free-flight test when the aircraft is unpowered, a critical factor for the carrier selection is the size of the airfield and the airspace that is required to perform the experiment, which depends on the drop altitude. For example, the Space Shuttle program included tests of the approach and landing phases of the unpowered orbiter (full-scale prototype), which was lifted by a modified B747 aircraft [22]. The orbiter was attached on the top of the carrier, and the separation procedure was designed based on the wind tunnel tests and simulations [22]. The orbiter was piloted by two onboard astronauts. Due to the size (weight) of the orbiter, neither the helicopter nor the balloon could be used as a suitable carrier. Using the aircraft as a carrier allows for achieving a higher altitude and higher Mach number. On the other hand, dropping a full-size prototype from an aircraft requires access to controlled aerospace and airfield, which are most likely accessible and affordable for big national agencies or big industrial concerns. The National Aeronautics and Space Administration (NASA) conducted numerous experiments, wherein the aircraft or its prototype was launched by dropping it from an airplane: for instance, the F15 scaled model was dropped from a B-52 aircraft [24], X38 was dropped from B-52 [20], and X43A was dropped from B-52 [25].

An example of the project in which the helicopter was used for the drop test of an unpowered prototype is the Dream Chaser rocket-plane. The unmanned prototype of this rocket-plane was lifted by the Erickson Air-Crane N164AC helicopter [26]. Moreover, helicopters were used by NASA in tests of

F-4 [7] and X-31 [23]. Another example of the use of a manned helicopter to drop a scaled model of a highly manoeuvrable aircraft is the flight campaign of F15 [7] and F/A-18E [21]. Helicopters also can be used as carriers in the case of the space capsule drop. However, such experiments are quite often related to testing the landing impact on a structure or the deployment of parachutes [27]; this is beyond the scope of this paper.

Balloons are typically used in the case of supersonic vehicle tests, when achieving a high altitude is crucial to ensuring that the aircraft can accelerate to a high speed. This kind of test can be conducted using stratospheric balloons filled with helium. Examples of such tests can be found elsewhere [18,28]. Again, this requires access to a quite large controlled aerospace [18]. Furthermore, in the case of a regular balloon, it is difficult to precisely control its movement against the ground. Moreover, the procedure of a launch is quite complex, which makes it a poor solution for a low-cost flight test campaign. Another carrier that should be mentioned here is a dirigible balloon; in the past, the United States used them to carry aircraft [29], but there are no records that such a vehicle was used in research flight tests as a carrier.

3. RESULTS

3.1. Flying model design

As a result, the rocket-plane model was built in a 1:10 scale with a semimonocoque structure, using the wet composite technology. The fuselage's and wing's skins were built as a sandwich structure using two layers of glass fibre (47 g/m^2), a foam (of 0.8 mm thickness) and two layers of glass fibre (47 g/m^2). All layers of glass fibre were oriented at 45°. The fuselage's inside structure was reinforced by carbon longerons and plywood frames (Fig. 2), while the wing's structure included ribs and spars. The size of the main spar was designed based on the shear force and the bending moment, calculated using the aerodynamic load computed by the MGAERO software [30]. The leading edge extension was exchangeable and built from 2.5 mm birch plywood. The side plates were built using balsa wood reinforced with carbon rods and covered with heat-shrinkable foil. The geometrical parameters of the model are presented in Table 2. To ensure good visibility and easy assessment of where the top and bottom parts of the model are, different colours of foil were used. The top side plates are yellow, while the bottom side plates are red (see Fig. 3). The different colours on the bottom and top parts are absolutely crucial in the case of a symmetrical model, in which judgement of the model orientation from a long distance can be difficult.

Table 2. The main geometrical features of the rocket-plane model.

Feature name	**Value**	**Unit**
Empty weight (without instrumentation and battery)	1.022	kg
Total weight without the balance mass	1.5	kg
Balance mass	0.1	kg
Wing area (without the LEX)	0.1884	m^2
Wingspan (without the side plates)	0.5	m
Wingspan	0.712	m

LEX, leading edge extension.

Figure 2. The rocket-plane model during the building process; the inside structure is glued into the composite skin [own study].

Figure 3. The rocket-plane model: view from a distance. The yellow and red colours were selected to ensure good visibility for the pilot and help to distinguish where the top and bottom of the model are [own study].

3.2. Concept of control

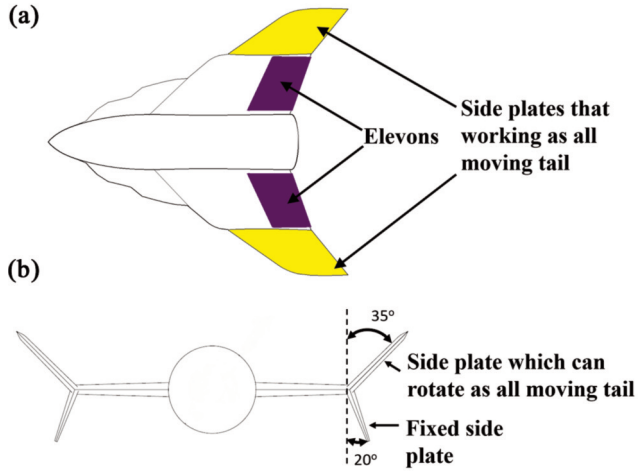

Figure 4. Concept of the rocket-plane control. Elevons can control the pitch and roll channel (a), while the side plates can control the pitch and yaw channel (b) [own study].

The rocket-plane model is designed in a tailless configuration, with the side plates installed on the wings' tips (Fig. 4). The plates are not perpendicular to the wing (see Fig. 4b); therefore, they affect

both longitudinal and directional motions. The pitch motion can be controlled by the elevons and/or symmetrical deflections of the side plates (Fig. 5). But when the side plates are deflected asymmetrically, then one can control the yaw motion. The mode of the side plates' deflections is controlled by a mixer.

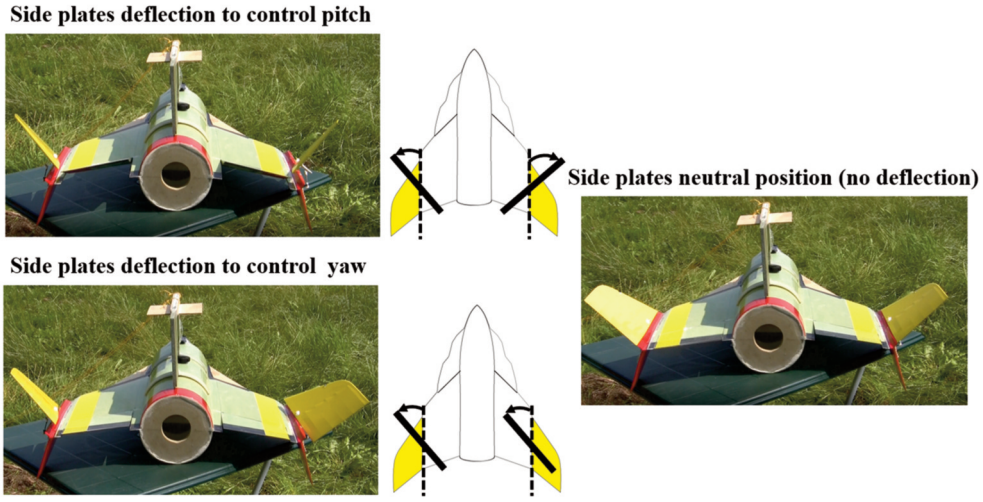

Figure 5. Possible ways of side plate deflection: symmetrical for longitudinal control (on the top left) and asymmetrical for directional control (on the bottom left) [own study].

The servomotors (HiTec HS-5125MG) responsible for upper plate rotation were installed in the bottom plates (Fig. 6, picture on the left), while the servomotors (HiTec HS-5085MG) controlling the elevons were installed in the wing (Fig. 6, picture on the right). Both servomotors are digital, and their specification can be found in Table 3.

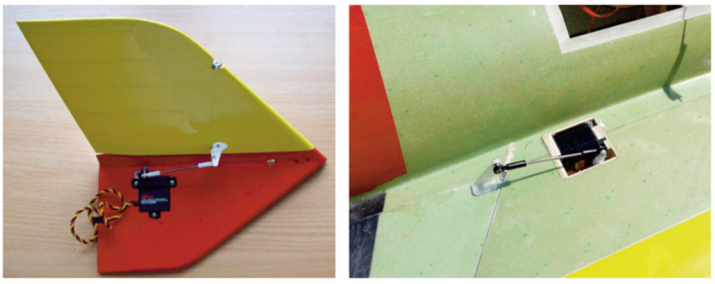

Figure 6. Servomotor installation on the side plates (on the left) and on the wing (on the right) [own study].

Table 3. Servospecificities of control surface servomotors.

Feature	**HiTec HS-5125MG**	**HiTec HS-5085MG**
Weight	24 g	21.9 g
Size (length/width/height)	30/34/10 mm	29/30/13 mm
Speed	0.13 s/60°	0.14 s/60°
Torque	4.0 kg cm	4.3 kg cm

3.3. Assembly element

To perform the drop tests, the manner of rocket-plane attachment to a carrier needed to be solved. A special component to hold the rocket-plane model was designed (Fig. 7). The assembly element was designed under the assumption that it can be used with different carriers, it must keep the rocket-plane in position ensuring that the path angle is equal to zero, and minimise the impact of the release process on the rocket-plane's motion. There is a single point where this holding element is mechanically connected with the rocket-plane model (Figs 7 and 8). The supports on the front and on the back ensure the proper positioning of the rocket-plane in the horizontal plane. The release mechanism uses a servomotor (HiTec HS-82MG), which actuator is connected to an off-the-shelf hook for radio-controlled (RC) gliders (see Fig. 8). The control signal to release the rocket-plane model is commanded by the rocket-plane pilot. The assembly element was built using the composite technology as a sandwich structure using fibre glass and 10 mm foam.

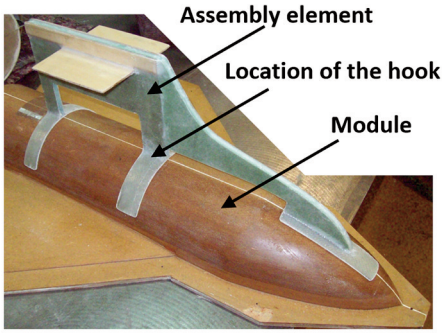

Figure 7. Holding element during the manufacture process [own study].

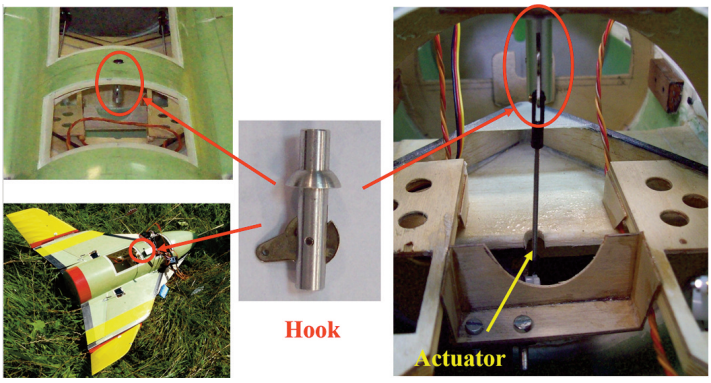

Figure 8. Hook [own study].

3.4. Instrumentation

The selection of technique for AoA measurements was the first challenge that needed to be addressed. The classic approach uses a sensor based on a potentiometer [31]. Such detection of the AoA by a sensor is based on the forces. However, for the drop with the airspeed around zero, the expected forces are going to be lower than the sensor's resolution. The second approach can be a five-hole pressure probe [32,33] (Fig. 9a), but the wind tunnel test reveals that for low speeds, the pressure

difference is also lower than the pressure sensor resolution. The probe was connected to the pressure sensor embedded in the Eagle Tree Universal Serial Bus (USB) Flight Data Recorder. The wind tunnel test showed that the measurement of an AoA is possible at speeds >5.8 m/s; the measured characteristics of the five-hole pressure probe are presented in a previous paper [14]. Therefore, an alternative technique for measurement of the AoA for very low airspeeds needs to be found. There was no sensor that could very precisely measure the AoA for such conditions; therefore, indicators were built by using a disc with a protractor and a thread attached in the centre (Fig. 10). Two indicators were installed, one for each wing (Fig. 10). The movement of each thread was recorded by a separate camera placed on the fuselage. The AoAs were extracted in the video postprocessing stage.

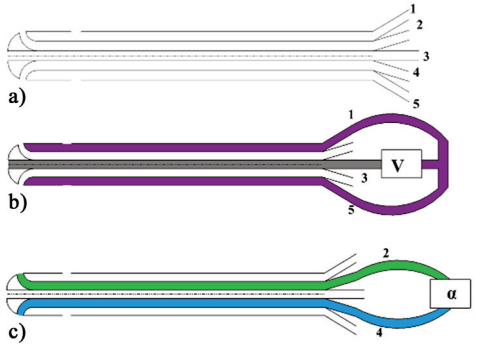

Figure 9. Five-hole pressure probe to measure the speed (calibrated airspeed) and angle of attack [own study].

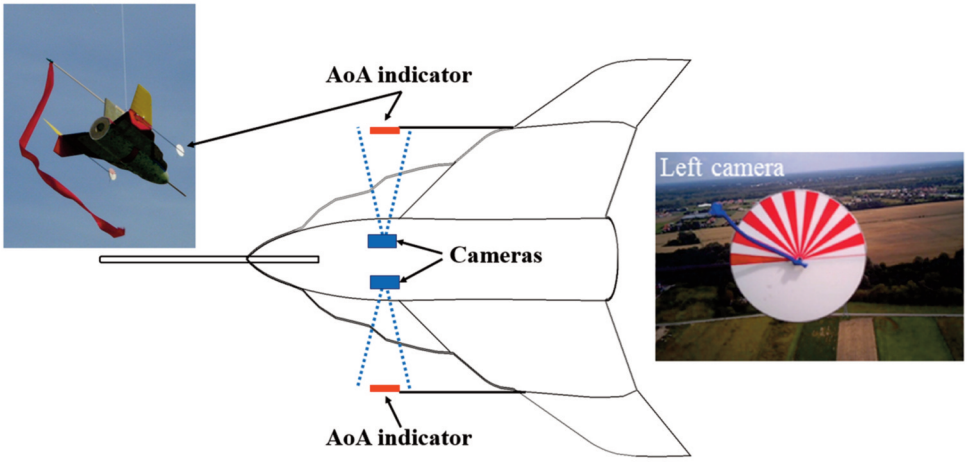

Figure 10. Arrangement of angles of attack (AoAs) indicators [own study].

The airspeed was also measured using two different sensors. The first one was based on the pressure difference obtained from the five-hole pressure probe (see Fig. 9b). The second type of sensor to measure the speed was a global positioning system (GPS)-based sensor. A similar approach was used for the altitude measurement: two sensors were integrated—one based on the pressure and the second using GPS readings. The last-measured parameters were the g-loads, which were measured by the accelerometer. The angular rates and attitude angles were not measured because the main emphasis of this experiment was to measure the *g*-forces and the rate of *g*-forces.

The rocket-plane model was equipped with three data loggers in total. The EagleTree E-logger V4 was connected to the GPS, accelerometer, barometric altitude sensor and servomotor of the release mechanism. The remaining flight parameters were recorded by the two EagleTree USB Flight Data Recorders. The first one registered the reading regarding the AoA from the five-hole pressure probe (see Fig. 9c) and the signal of the servomotors, which controlled the side plates and the release mechanism. The second Eagle Tree USB Flight Data Recorder recorded the reading from the five-hole pressure probe regarding the airspeed (see Fig. 9b) and the signal of the servomotors that controlled the elevons and the release mechanism. The reason behind the recording of the release mechanism signal was to synchronise the data from all loggers in the postprocessing stage. All parameters were recorded with a frequency of 10 Hz, which is not a high frequency, but the initial analysis of the model using the SDSA software [10] revealed that the duration of the short period oscillation is about 0.77 s. Considering this flight campaign as a low-cost experiment, using the instruments available at the University, this precision level was decided as acceptable.

3.5. Using a kite as a model carrier

The kite used in the experiment was a very stable photographic platform, but the minimum wind speed needed to launch it was about 7 m/s. To ensure the safety of the rocket-plane model during the launch of the kite, the model stayed on the ground until the kite was in the right position; then, the model was lifted using a pulley-block system (Fig. 11, picture on the right). But before the actual rocket-plane model was used, the system was tested with a dummy load to ensure that the kite can lift a weight that is bigger than the weight of the rocket-plane model. The picture of the rocket-plane model and kite before the model release is presented in Fig. 11 (picture on the left).

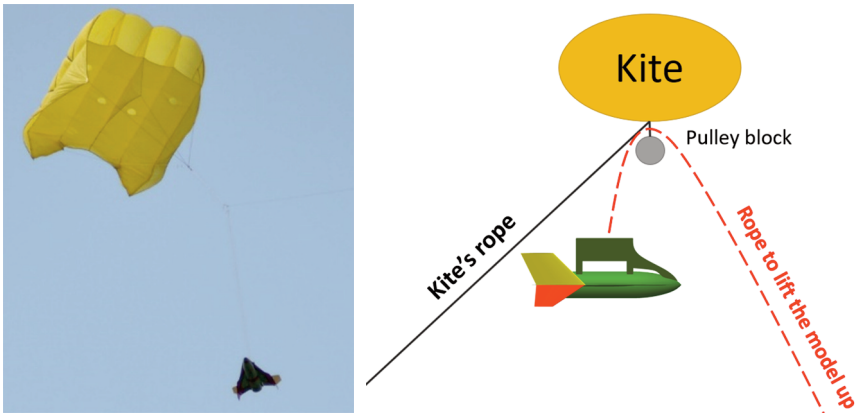

Figure 11. The rocket-plane hanging to the kite before the release (on the left), scheme of system connection (on the right) [own study].

Because the minimum wind speed was close to the stall speed of the rocket-plane model, this could compromise the experiment's assumption that the drop is to be performed for an initial speed lower than the stall airspeed. Moreover, the success of the kite launch and the maximum altitude were very strongly connected to the weather condition. Furthermore, the preparation time required to launch the kite and the launching process itself were very time-consuming, which later on affected the decision to change the carrier vehicle. During the flight test campaign, two drops from the kite were performed. The sequence of pictures recorded by the camera after the release is presented in Fig. 12; the camera was attached to the holding element. When the rocket-plane model was very close to the kite, a strong

oscillation caused by the aerodynamic interference was observed. Another issue was the relatively low maximum altitude that the kite was able to achieve.

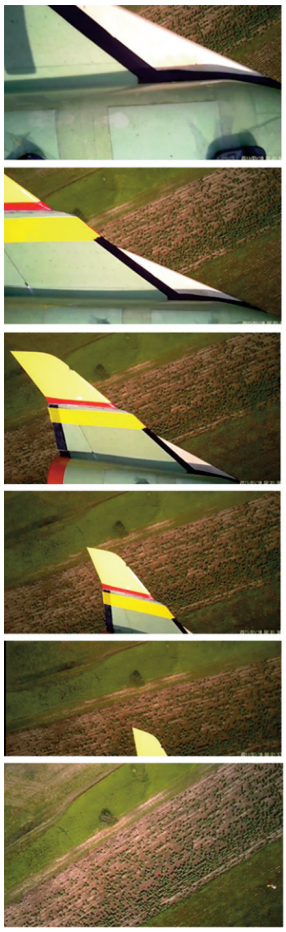

Figure 12. Sequence of pictures recorded by the camera after the model was dropped from the kite [own study].

3.6. Using a UAV helicopter as a model carrier

Eventually, due to the very long time of preparation and the strong link of the experimental condition to the weather, the decision was made to use a different vehicle as the carrier. The lesson learned from the kite test confirmed that the rocket-plane model cannot be too close to the carrier because of strong aerodynamic interference. To avoid that problem, the holding element must be attached on a long rope (10 m), which implies that the model of the rocket-plane might behave like a pendulum during the forward flight of the whole system. Both the UAV quadcopter and the UAV helicopter—as the carrier—were analysed. The flight campaign was performed in 2014 when the autopilots of quadcopters were not very advanced. For stability in this experiment, the system was required to handle the situation that, during the flight, the position of the centre of gravity (CG) changed. This is expected to occur because the rocket-plane model is attached through the rope and can affect the CG by the pendulum motion. But at the time there was not a suitable UAV helicopter

on the market capable to perform such a mission. Therefore, it was decided that a skilled pilot should be able to handle such a flight, but by flying using a UAV helicopter that is not equipped with an advanced stabilisation system, the T-Rex 700N helicopter fulfils this requirement. To mitigate the effect of the rocket-plane model on the CG, the rope was attached to the helicopter's CG. The modification that was implemented after the kite test included adding a stick and a ribbon to the rocket-plane's holding element (see Fig. 13) to improve the system's stability and mitigate the model's spinning.

Figure 13. On the left, initial configuration of the holding component (without the ribbon). In the middle and on the right, the modified version of the holding element is shown with the stick and the ribbon [own study].

3.7. Preflight, takeoff and flight procedures

The first few flights were performed to set the aircraft's CG in appropriate position. Finally, 100 g extra mass must be taken on board to ensure the right mass distribution. This position was marked on the rocket-plane model to ensure that the CG position is the same in the whole flying test campaign. The setting of the CG was the first step. The preflight procedure consisted of connecting all electronics with batteries and switching them on and checking the radio connections, including deflections of control surfaces. Next, the whole system was connected, starting with the helicopter, the assembly element with the rope and rocket-plane model.

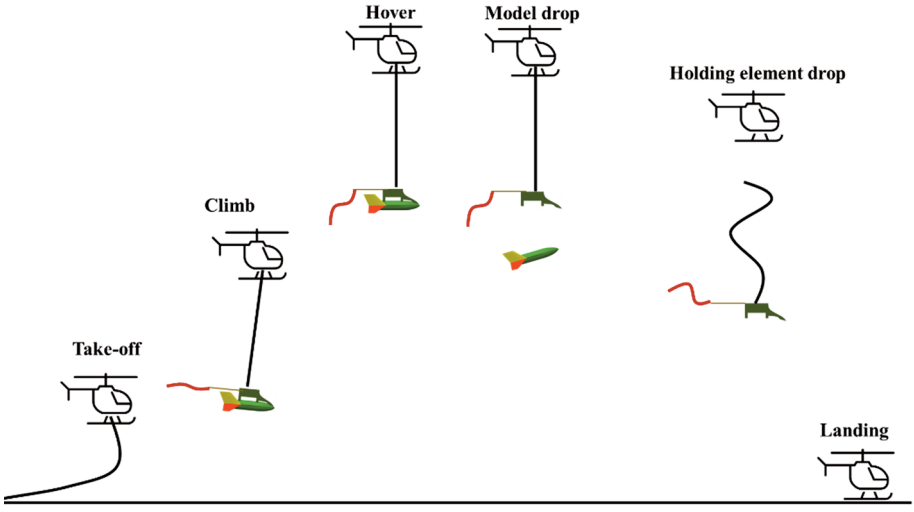

Figure 14. Procedure of the experiment from the helicopter operator's point of view [own study].

The schemes of the flight procedure from the helicopter operator's point of view and from the rocket-plane operator's point of view are presented in Figs 14 and 15. The pictures of the rocket-plane model before and after separation are presented in Fig. 16, and those taken during the standalone flight are shown in Fig. 17. The postflight procedure included extracting the data from the data loggers and copying the movies from the cameras.

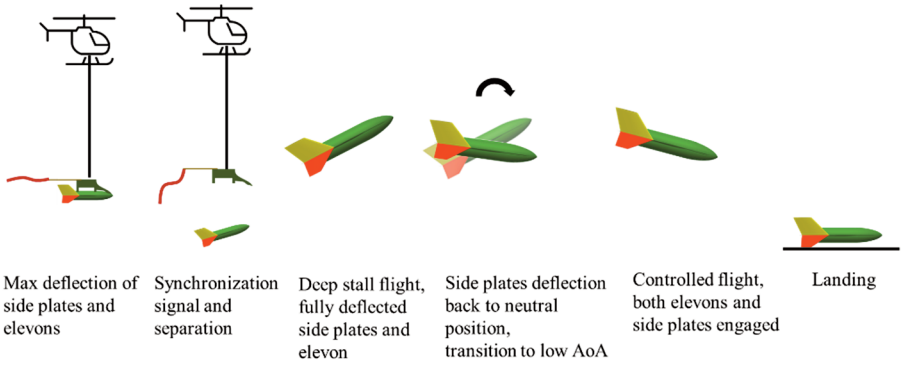

Figure 15. Procedure of the experiment from the rocket-plane operator's point of view [own study].

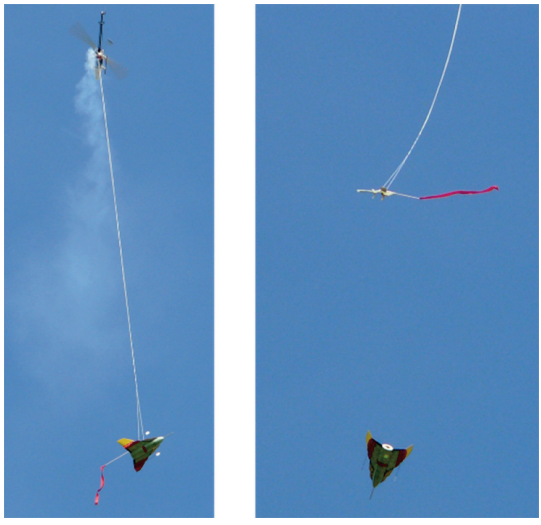

Figure 16. Model before the separation (on the left) and after separation (on the right) [own study].

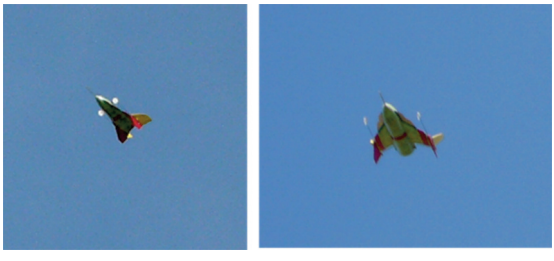

Figure 17. The rocket-plane model in standalone flight [own study].

An exemplary set of data recorded during one of the flights is presented in Fig. 18; more results, with the corresponding analysis, can be found in a previous paper [14].

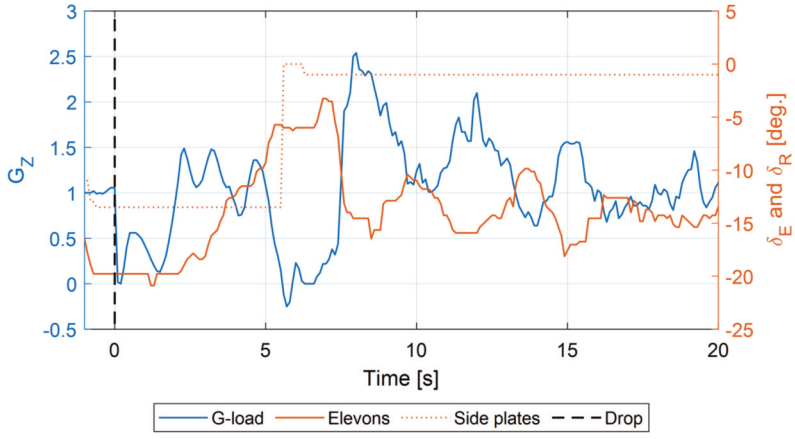

Figure 18. Example of *g*-load and movement of the elevons and side plates recoded during one of the flights. Time =0 represents the moment of the rocket-plane drop.

4. DISCUSSION

Using an UAV helicopter rather than the kite is more appropriate when the airspeed for the drop must be very close to zero. Moreover, in the case of the UAV helicopter, the altitude of the experiment can be higher and the procedure of takeoff is more efficient. Moreover, there is better control of where exactly the model drop occurs. The herein-presented technique of conducting the free-flight test is especially suitable for unpowered vehicles or for a test wherein the engine(s) failure is going to be simulated. This type of free-flight tests involves relatively low cost, which is a good opportunity for universities or for the early-stage design process, when expensive flight tests are not needed yet. However, flying a helicopter with an attached model on a long rope requires a very skilful helicopter pilot (Fig. 16). The challenge is limited not only to the part of the flight when the model is attached but also when there is only the holding element, because, in this phase, there is a bigger probability that the rope can become entangled with the helicopter's rotor. To ensure a safe landing of the helicopter, a releasing mechanism for the rope was implemented. An additional stabilisation element was attached to the assembly element to avoid spinning of the rocket-plane model. The ribbon on the stick was sufficient to solve this problem.

The flying technique of the rocket-model airplane under below-stall conditions is very challenging, as the aerodynamic controls are not effective in such flight conditions. Therefore, a special configuration of the rocket-model control surfaces has been devised for below-stall airspeed range (Fig. 15). The configuration was especially developed to ensure stable high AoA during descent in both below- and beyond-stall speed ranges. When the model airspeed increased to provide sufficient authority to control surfaces, the AoA was decreased appropriately to allow high-speed gliding. Because of the model size and high-speed flight due to the relatively high wing loading, the airplane control in such condition requires a well-skilled radio control (RC) pilot.

Due to the large number of sensors used, >1 data logger was required. Having data set files from different loggers caused an issue with data synchronisation. Therefore, to eliminate this problem, one common signal was recorded by all loggers. This helped to synchronise the data in the postprocessing stage; the synchronisation signal was commanded by the rocket-plane operator just before the separation.

5. CONCLUSIONS

In this paper, a lesson learned from the rocket-plane model free-flight tests is presented. The description of the process of model building, planning of the experiment, model preparation and operation procedure are presented. To successfully perform free-flight tests, the following problems must be addressed:

- Can a model be dynamically scaled and which similarity numbers must be met?
- How to launch a model and what kind of carrier vehicle is the most appropriate?
- What kind of data is going to be measured and how?

Owing to the use of the UAV helicopter, the operation procedure and the cost of the flight campaign were significantly reduced. However, because the rocket-plane model did not meet the Froude scale (it was not a dynamically scaled model), the data recorded by such a mode cannot be directly used to represent the behaviour of the full-scale rocket-plane. However, the data can be used to validate numerical software in terms of general modelling of flight in a deep stall condition; this is presented in previous work [14]. The instruments that the model was equipped with measured the airspeed, g-force and AoA. This satisfied all experimental requirements listed in Section 2.1.

In general, utilisation of a UAV helicopter as a carrier could be a good opportunity for universities or for the early-stage design process, when expensive flight tests are not needed yet. However, the drawback of the presented method is that such an approach requires two pilots, one for the carrier and one for the tested airplane.

Acknowledgments: The building of the flying model and the flight test campaign were supported by the Zonta International Amelia Earhart Fellowship Program. We extend special thanks to all the numerous volunteers who helped in conducting this research but were not qualified as coauthors.

REFERENCES

[1] Figat, Marcin., Galiński, Cezary. and Kwiek, Agnieszka. "Modular Aeroplane System. A Concept and Initial Investigation." *Proceeding of ICAS 2012 Conference*, Brisbane, paper number ICAS 2012-1.3.2, paper no ICAS 2012-1.3.2 (2012).

[2] Figat, Marcin. and Kwiek, Agnieszka. "Aerodynamic and Static Stability Investigation into Aircraft Coupled System to Suborbital Space Flights." *Aircraft Engineering and Aerospace Technology* Vol. 93 No. 2 (2021): pp. 275–283. DOI 10.1108/AEAT-05-2020-0085.

[3] Galiński, Cezary., Goetzendorf-Grabowski, Tomasz., Mieszalski, Dawid. and Stefanek, Łukasz. "A Concept of Two-Staged Spaceplane for Suborbital Tourism." *Transactions of the Institute of Aviation* Vol. 191 No. 4 (2007): pp. 33–42.

[4] Antuñano, Melchor., Baisden, Denise., Davis, Jeffrey., Hastings, John., Jennings, Richard., Jones, David, Jordan, Jon, Mohler, Stanley., Ruehle, Charles., Salazar, Guillermo., Silberman, Warren., Scarpa, Phillip., Tilton, Frederick. and Whinnery, James. "Guidance for Medical Screening of Commercial Aerospace Passengers." FAA report DOT/FAA/AM-06/1 (2006): Available at https://libraryonline.erau.edu/online-full-text/faa-aviation-medicine-reports/AM06-01.pdf (accessed on 10.01.2021).

[5] Galiński, Cezary. and Goraj, Zdobysław. "Experimental and Numerical Results Obtained for A Scaled RPV and A Full Size Aircraft." *Aircraft Engineering and Aerospace Technology* Vol. 76 No. 3 (2004): pp. 305–313. DOI 10.1108/00022660410536041.

[6] Kimberlin, Ralph. *Flight Testing of Fixed Wing Aircraft*. American Institute of Aeronautics and Astronautics, Reston, VA (2003).

[7] Chambers, Joseph. *Modeling Flight. The Role of Dynamically Scaled Free-Flight Models in Support on NASA's Aerospace Programs*. U.S. Government Printing Office, Washington DC (2009).

[8] Galiński, Cezary., Bartkiewicz, Piotr., Hajduk, Jarosław. and Lamers, Piotr. "Results of the J-5 Marco Dynamic Similar Model Flight Tests Program." SAE Paper No. 975551, 1997 World Aviation Congress, 1316.10.1997, Anaheim, CA (1997).

[9] Wolowicz, Chester., Bowman, James Jr. and Gilbert, William. Similitude Requirements and Scaling Relationships as Applied to Model Testing." NASA Technical Paper 1436.

[10] SDSA – Simulation and Dynamic Stability analysis, Warsaw University of Technology, Available at www.meil.pw.edu.pl/add/ADD/Teaching/Software/SDSA (accessed on 16.12.2021).

[11] Goetzendorf-Grabowski, Tomasz., Marcinkiewicz, Ewa. and Galiński, Cezary. "Comparison of Traditionally Calculated Stability Characteristics with Flight Test Data of PW-6U sailplane." *Proceedings of the CEAS Conference*, pp. 536–543. Linköping, Sweden, 15–19.09.2013. Linköping University Electronic Press, Linköping (2013).

[12] Goetzendorf-Grabowski, Tomasz. and Antoniewski, Tomasz. "Three Surface Aircraft (TSA) Configuration – Flying Qualities Evaluation." *Aircraft Engineering and Aerospace Technology*, Vol. 88 No. 2 (2016): pp. 277–284. DOI 10.1108/AEAT-02-2015-0055.

[13] Mieloszyk, Jacek., Tarnowski, Andrzej., Tomaszewski, Adam. and Goetzendorf-Grabowski, Tomasz. "Validation of Flight Dynamic Stability Optimization Constraints with Flight Tests." *Aerospace Science and Technology* Vol. 106, (2020): DOI 10.1016/j.ast.2020.106193.

[14] Kwiek, Agnieszka., Galiński, Cezary., Bogdański, Krzysztof., Hajduk, Jarosław. and Tarnowski, Andrzej. "Results of Simulation and Scaled Flight Tests Performed on A Rocket-Plane at High Angles of Attack." Aircraft Engineering and Aerospace Technology Vol. 93 No. 9, (2021): pp. 1445–1459. DOI 10.1108/AEAT-11-2020-0276.

[15] Galiński, Cezary. and Hajduk, Jarosław. "Assumptions of the Joined Wing Flying Model Programme." *Transactions Of The Institute of Aviation* Vol. 238 No. 1 (2015): pp. 7–21.

[16] Jouannet, Christopher., Berry, Patrick., Melin, Tomas., Amadori, Kristian., Lundström, David. and Staack, Ingo., "Subscale Flight Testing used in Conceptual Design." *Aircraft Engineering and Aerospace Technology* Vol. 84 No. 3 (2012): pp. 192–199. DOI 10.1108/00022661211222058.

[17] Lundström, David., Sobron, Alejandro., Krus, Petter., Jouannet, Christopher., Gil Annes da Silva, R. "Subscale Flight Testing Of A Generic Fighter Aircraft." *30th International Congress Of Aeronautical Sciences* 25–30 Spetember 2016, Daejeon, Korea, paper No 2016_0390 (2016).

[18] Yanagihara, Masaaki. and Munenaga, Takao. "High Speed Flight Demonstration Project", *24th International Congress of Aeronautical Sciences*, 29 August–3 September 2004, Yokohama, Japan, Paper No ICAS 2004-7.1.1 (I.L.) (2004).

[19] Goraj, Zdobysław., Malinowski, Marek. and Frydrychewicz, Andrzej. "Design of Novel Aerial Jet Target." *Aircraft Engineering and Aerospace Technology* Vol. 89 No. 4 (2017): pp. 511–519. DOI 10.1108/AEAT-10-2016-0174.

[20] Banks Daniel. and Fisher David. "Aft-End Flow of a Large-Scale Lifting Body During Free-Flight Test." NASA/TM-2006-213681 (2006).

[21] Croom, Mark., Kenney, Holly., Murri, Daniel. and Lawson, Kenneth. "Research on the F/A-18E/F Using a 22%-Dynamically-Scaled Drop model." *AIAA Atmospheric Flight Mechanics Conference and Exhibition*, 14–17 August 2000, Denver, Colorado (2000).

[22] Homan, D.J. Denison D.E. and Elchett, K.C. "Orbiter/Shuttle Carrier Aircraft Separation: Wind Tunnel, Simulation, and Flight Test Overview and Results." NASA Technical Memorandum 58223 (1980).

[23] Klein, Vladislav. and Noderer Keith. "Aerodynamic Parameters of the X-31 Drop Model Estimated from Flight-Data at High Angles of Attack." *Guidance, Navigation and Control Conference* 10–12.08.1992, Hilton Head Island, SC, U.S.A., AIAA-92-4357CP (1992).

[24] Iliff, Kenneth., Maine, Richard. and Shafer, Mary. "Subsonic Stability and Control Derivatives for an Unpowered, Remotely Piloted 3/8-Scale F-15 Airplane Model Obtained from Flight Test." NASA Technical Note TN D-8136 (1976).

[25] Lux Jessica. and Burkes Darryl. "Hyper-X (X-43A) Flight Test Range Operations Overview." NASA/TM-2008-214626 (2008).

[26] NASA. https://www.nasa.gov/exploration/commercial/crew/snc_captivecarry.html (accessed on 12.01.2022).

[27] Evans, Carol. *Orion Capsule Parachute Assembly System (CPAS) Airdrop Test Program Techniques, Challenges, and Solutions*. AIAA Aviation and Aeronautics Forum, Dallas, TX (2019).

[28] Honda Masahisa. and Yoshida Kenji. "D-SEND#2 Flight Demonstration for Low Sonic Boom Design Technology." 2014, *29th International Congress of Aeronautical Sciences*, 7–12 September 2014, St. Petersburg, Russia, Paper No ICAS2014_0505 (2014)

[29] Grossnick, Roy. *Kite Balloons to Airship: the Navy's Lighter than Air Experience*. Published by the Deputy Chief of Naval Operations (Air Warfare) and the Commander, Naval Air System Command, Washington D.C. (1987).

[30] Analytical Methods, INC., MGAERO user's manual Version 3.1.4., Redmond, Washington USA, 1990-2001

[31] Corda, Stephen. and Vachon, Michael. "Design and Flight Evaluation of a New Force-Based Flow Angle Probe." NASA Technical Memorandum NASA/TM-2006-213673 (2006).

[32] Bennett, Donald. "Evaluation of Hemispherical Head Flow Direction Sensor for Inlet Duct Measurements." NASA TMX-3232, (1975): Available at: www.nasa.gov/centers/dryden/pdf/87861main_H-862.pdf (accessed 10.01.2022).

[33] Gonzalez, Jose. and Arrington, Allen. "Five-Hole Flow Angle Probe Calibration for the NASA Glenn Icing Research Tunnel." NASA/CR-1999-202330 (1996). Available at: https://ntrs.nasa.gov/archive/nasa/casi.ntrs.nasa.gov/19990047776.pdf (accessed 10.01.2022).